Cerebral Cortex, 2018; 1–16

doi: 10.1093/cercor/bhy005
Original Article

ORIGINAL ARTICLE

Genetic Influences on the Development of Cerebral Cortical Thickness During Childhood and Adolescence in a Dutch Longitudinal Twin Sample: The Brainscale Study

Jalmar Teeuw[1], Rachel M. Brouwer[1], Marinka M.G. Koenis[1], Suzanne C. Swagerman[2], Dorret I. Boomsma[2] and Hilleke E. Hulshoff Pol[1]

[1]Department of Psychiatry, Brain Center Rudolf Magnus, University Medical Center Utrecht, Heidelberglaan 100, 5384 CX Utrecht, the Netherlands and [2]Department of Biological Psychology, Vrije Universiteit Amsterdam, van der Boechorststraat 1, 1081 BT Amsterdam, the Netherlands

Address correspondence to Hilleke E. Hulshoff Pol, Department of Psychiatry, Brain Center Rudolf Magnus, University Medical Center Utrecht, Heidelberglaan 100, 5384 CX Utrecht, the Netherlands. Email: H.E.Hulshoff@umcutrecht.nl

Abstract

Previous studies have demonstrated that cortical thickness (CT) is under strong genetic control across the life span. However, little is known about genetic influences that cause changes in cortical thickness (ΔCT) during brain development. We obtained 482 longitudinal MRI scans at ages 9, 12, and 17 years from 215 twins and applied structural equation modeling to estimate genetic influences on (1) cortical thickness between regions and across time, and (2) changes in cortical thickness between ages. Although cortical thickness is largely mediated by the same genetic factor throughout late childhood and adolescence, we found evidence for influences of distinct genetic factors on regions across space and time. In addition, we found genetic influences for cortical thinning during adolescence that is mostly due to fluctuating influences from the same genetic factor, with evidence of local influences from a second emerging genetic factor. This fluctuating core genetic factor and emerging novel genetic factor might be implicated in the rapid cognitive and behavioral development during childhood and adolescence, and could potentially be targets for investigation into the manifestation of psychiatric disorders that have their origin in childhood and adolescence.

Key words: cortex, development, heritability, plasticity, twins

Introduction

The human brain changes substantially during development from fetus to newborn to adult. Noninvasive magnetic resonance imaging (MRI) has enabled the study of brain structure and function in healthy children and adolescents. Brain imaging studies from the past two decades have documented the changes that occur to the brain during development from childhood into early adulthood (Giedd et al. 2010). The size of the brain of an 9-year-old child is already at approximately 96% of its maximum size (Dekaban and Sadowsky 1978; Hedman et al. 2011), but continues to develop as the child transitions through adolescence and matures into adulthood. For example, total grey matter volume starts to decrease around the start of puberty, while total white matter volume continues to increase well into adulthood (Giedd et al. 1999; Mills et al. 2016). This reduction in total grey matter volume and increasing myelination of white matter connections

in the brain is accompanied by an apparent decrease in grey matter cortical thickness during adolescence. Characterizing brain development in healthy children and adolescents is essential to understand when and how development is stunted in atypically developing children. Divergence from typical developmental trajectories has been associated with increased liability for psychiatric disorders (Greenstein et al. 2006; Shaw et al. 2007; Paus et al. 2008; Rapoport and Gogtay 2008; Zielinski et al. 2014; Giedd et al. 2015). Indeed, developmental trajectories and their underlying processes may be more informative about vulnerability for disease and clinical outcomes than absolute measures (Paus et al. 2008; Shaw et al. 2010; Schnack et al. 2015; 2016), highlighting the importance of longitudinal cohorts in developmental studies (Mills and Tamnes 2014).

The inclusion of twins in brain imaging studies has provided valuable information about the influences of genes and environment on brain development (Peper et al. 2007; Blokland et al. 2012; den Braber et al. 2013; Douet et al. 2014; Jansen et al. 2015; Strike et al. 2015). Twin studies allow us to unravel genetic influences on the architecture of the brain and explain to what extent variation in brain measures are heritable, i.e., the extent to which individual differences can be attributed to genetic factors, or to common and unique environmental factors. The classical twin model allows for the study of genetic influences on the human brain by measuring similarities between monozygotic and dizygotic twins (Posthuma et al. 2000; Boomsma et al. 2002). Heritability estimates have revealed that most of the brain's structure is under genetic control (Peper et al. 2007; Blokland et al. 2012; Douet et al. 2014; Strike et al. 2015). Cortical thickness is found to have moderate to strong heritability (Thompson et al. 2001; Hulshoff Pol et al. 2006; van Soelen et al. 2012b) and heritability of cortical thickness is suggested to increase with age (Lenroot and Giedd 2008; Schmitt et al. 2014). To date, there are few longitudinal studies which allow estimation of genetic influences on "changes in cortical thickness" (Brans et al. 2010; van Soelen et al. 2012b; Hedman et al. 2016). We previously found evidence for heritability of cortical thinning in children between the ages 9 and 12 years (van Soelen et al. 2012b). Of interest, at age 12 years, we found genetic innovation for cortical thickness in a prefrontal region, indicating that novel genetic factors become involved in the development of cortical thickness around the start of puberty. However, little is known about the dynamic landscape of genetic and environmental influences on cortical development during adolescence, a period with large cognitive and behavioral changes and a critical period for the manifestation of psychiatric disorders. In the current study, we report on the development of cortical thickness in the BrainSCALE twin cohort for which we measured the twins again at age 17 years, bringing the number of repeated assessment to three. We investigated the spatiotemporal dynamics of genetic and environmental influences on cortical thickness. Specifically, we address the question whether different genetic factors influencing cortical thickness at different stages of childhood and adolescent brain development. Using twin modeling, we estimated genetic correlations between cortical regions to assess "spatial genetic differentiation" between regions within the same age and "temporal genetic differentiation" between regions at different ages. In addition, we extend on our previous findings on heritability of changes in cortical thickness between age 9 and 12 years (van Soelen et al. 2012b) with new finding on heritability of changes in cortical thickness between age 12 and 17 years. We have included new estimates of our previous finding between age 9 and 12 years given the increase in power to detect smaller effect sizes with greater accuracy by including the third measurement.

Materials and Methods

Participants

A total of 112 families consisting of twin pairs born in 1995–1996 and their older siblings, were invited to participate in the longitudinal BrainSCALE study on brain and cognitive development during childhood and adolescence (van Soelen et al. 2012a), a collaborative project between Netherland Twin Register (Boomsma et al. 2006; van Beijsterveldt et al. 2013) at the Vrije Universiteit (VU) Amsterdam and University Medical Center Utrecht (UMCU). The BrainSCALE cohort is a representative sample of mostly Caucasian typically developing children from the Dutch population. The twins were around 9 years of age when they were assessed with a battery of cognitive tests and extensive MRI protocol at baseline measurement (Peper et al. 2009). Two follow-up measurements were conducted when the twins were around 12 and 17 years of age. Here we report results on a subsample of the BrainSCALE cohort that includes all twins. A total of 482 MRI scans from 215 participants (111 females and 104 males; approximately 16% nonright-handed) between age 9 and 18 years were available for analysis (see also Supplementary Table S1). Structural MRI scans were acquired for most of the subjects participating in the BrainSCALE study (94%, 78%, and 98%, respectively, for each measurement; Supplementary Fig. S1). The decline in scan acquisition percentage at age 12 years was mostly due to exclusion of participants with dental braces incompatible with the magnetic field of the MR scanner. Other reasons for not acquiring scans include reluctance to participate and incomplete scans. In addition, a fraction of the acquired scans could not be processed due to scanning artefacts primarily related to head motion (9%, 9%, and 4%, respectively, for each measurement).

The study was approved by the Central Committee on Research Involving Human Subjects of The Netherlands (CCMO), and studies were performed in accordance with the Declaration of Helsinki. Parents signed informed consent forms for the children and for themselves. Children signed their own informed consent forms at the third measurement. Parents were financially compensated for travel expenses, and children received a present or gift voucher at the end of the testing days. In addition, a summary of cognition scores and a printed image of their T1 brain MRI scan, when available, were provided afterwards.

MRI Acquisition

Participants underwent medical resonance imaging (MRI) on a 1.5 Tesla Philips Achieva scanner (Philips, Best, Netherlands) at the University Medical Center Utrecht (UMCU). For brain anatomy, a three-dimensional T1-weighted scan (Spoiled Gradient Echo; TE = 4.6 ms; TR = 30 ms; flip angle = 30°; 160–180 contiguous coronal slices of 1.2 mm; in-plane resolution of 1.0 × 1.0 mm^2; acquisition matrix of 256 × 256 voxels; field-of-view of 256 mm with 70% scan percentage) of the whole head was acquired for each participant. The same scanners and scan sequence parameters were used at baseline and follow-up measurements to minimize the effect of differences in scan acquisition between measurements.

Image Processing

Images were re-oriented to Talairach space without scaling, and corrected for inhomogeneities in the magnetic field (Sled

et al. 1998). Quantitative assessment of intracranial volume (ICV) was performed as previously described for baseline (Peper et al. 2008) and follow-ups (van Soelen et al. 2013). Brain tissue was segmented into cerebrospinal fluid, grey matter and white matter using a partial volume segmentation algorithm that incorporates a nonuniform partial volume distribution (Brouwer et al. 2010). Cortical thickness was determined using a customized version of the CLASP algorithm designed at the McConnell Brain Imaging Centre, Montreal (Kim et al. 2005; Lerch et al. 2008). The grey and white matter segments obtained from our own partial volume segmentation algorithm were used to initialize the CLASP algorithm. A 3D surface was fitted to the white matter/grey matter interface to obtain the inner surface of the cortex. The outer cortical surface was obtained by expanding the inner surface outward until it fitted the grey matter/cerebrospinal fluid interface (Kim et al. 2005). Cortical thickness was defined at each vertex (40 962 vertices per hemisphere) as the distance between the two surfaces. Changes in cortical thickness between ages were computed by taking the difference in estimates and converted to change in millimeter per year by dividing the difference by the scan interval between the ages in years. Cortical thickness measures were smoothed across the surface using a 20-mm full-width-at-half-maximum (FWHM) surface-based blurring kernel. This method of blurring simultaneously improves the chances of detecting population differences and follows the curvature of the surface to preserve any anatomical boundaries within the surface. The surfaces of the individuals were registered to an average surface (ICBM average surface template; Lyttelton et al. 2007) to allow for comparison between and within subjects across age. Nonsmoothed cortical thickness mapped to ICBM average surface was used to compute mean cortical thickness for the major cortical lobes (frontal, parietal, temporal, and occipital lobes) and adjacent regions (insula and cingulate) obtained from the atlas provided by the CIVET software. The version of CIVET used in the analysis does not incorporate a dedicated longitudinal pipeline for simultaneous registration and classification of brain tissue. Nevertheless, cortical thickness estimates obtained using CIVET show high test-rest reliability (Jeon et al. 2017; Lewis et al. 2017), and a direct comparison of CIVET to FreeSurfer's longitudinal pipeline revealed no significant differences in effect sizes (Redolfi et al. 2015).

Linear Regression Modeling

Longitudinal mixed-effects models with cubic, quadratic, and linear age effects were fitted to the cortical thickness estimates while allowing for random intercept for individuals using the *nlme* package (Pinheiro et al. 2017) in R. The most parsimonious model was selected based on the log-likelihood ratio test.

Genetic Twin Modeling

Twin modeling can provide information on the variation of a trait in the population that can be explained by genetic factors (Posthuma et al. 2000; Boomsma et al. 2002). Based on the assumption that monozygotic twins share 100% of their genetic material and dizygotic twins share on average 50% of their segregating genes, the phenotypic variance (V) of a trait is usually decomposed into 3 independent variance components: additive genetic (A), common environmental (C), and unique environmental (E) components of variance. Additive genetic influences represent effects of multiple alleles at different loci across the genome that act in conjunction on the phenotypic trait. Common environmental influences represent sources of variance that are shared between twins of the same family and cause the twins to be more alike than children growing up in different families. Unique environmental influences are not shared by family members and may include measurement error (Falconer and Mackay 1996; Boomsma et al. 2002). If monozygotic twins resemble each other more than dizygotic twins for a given trait, then this difference is usually attributed to genetic influences. If both monozygotic and dizygotic twins are more alike in resemblance than expected based on genetics, common environmental influences are thought to play a role. Residual variation between twin pairs is attributed to unique environmental influences.

Structural Equation Modeling

Within structural equation modeling (SEM), the variance in univariate or multivariate phenotypes can be modeled as the combined effect of additive genetic factors, and common and unique environmental factors. These factors are modeled as latent variables with unit variance where path coefficients or factor loadings a, c, and e quantify their respective influence on the phenotypic trait(s). The model is made identifiable by putting constraints on the correlation $\rho_{\tilde{A}}$ between the latent variable $\tilde{A}$ of twin pairs; $\rho_{\tilde{A}}$=1.0 for monozygotic twins, and $\rho_{\tilde{A}}$=0.5 for dizygotic twins. The correlation $\rho_{\tilde{C}}$ between latent variable $\tilde{C}$ of members of a twin pair is constrained to $\rho_{\tilde{C}}$=1.0 for both monozygotic and dizygotic twins. The latent variable $\tilde{E}$ is uncorrelated between individuals within and across twin pairs. The sum of the squared path coefficients a^2, c^2, and e^2, representing the variance components A, C, and E, is equal to the phenotypic variance (V); i.e., $V = A + C + E = a^2 + c^2 + e^2$. Heritability ($h^2$) of the trait is estimated as the proportion of phenotypic variance (V) that is due to additive genetic variance (A); i.e., $h^2 = A/V = a^2/(a^2 + c^2 + e^2)$.

Nested models can be obtained by constraining parameters of interest in the model. Testing significance of nested models is performed using the log-likelihood ratio test. Statistical significance was determined by comparing the likelihood of the model fits from the model with and without a constraint on the parameter of interest. The difference in −2 times the log likelihood (−2LL) follows a χ^2 distribution. For variance components (e.g., heritability estimates, but not correlations), −2LL asymptotically follows a 50:50 mixture of χ^2 distributions with zero and one degree of freedom; effectively allowing p-values to be cut in half (Dominicus et al. 2006).

Structural equation models were defined using OpenMx version 2.2.6 (Boker et al. 2015), a package for structural equation modeling in R (R Core Team 2015). Model fitting was performed using full-information maximum likelihood (FIML) to take advantage of all available information in case of missing data. For example, when no data is available for one of the twins in a pair at any age, thereby creating a singleton "twin" at any or all three ages, FIML can still use the information from the available twin to improve the estimates of means and variances, thereby improving the overall fitting of the model parameters.

Based on our previous work (van Soelen et al. 2012b) and the fact that evidence for common environmental influences on cortical thickness is limited in the literature, we assume that common environment latent variable ($\tilde{C}$) could be dropped from our model. Indeed, based on the log-likelihood and Akaike Information Criterion, the longitudinal AE model fitted the cortical thickness measurements better than ACE, CE, or E on the global and lobar level (see Supplementary Table S2). We therefore adopted the AE model in all analyses.

Longitudinal Twin Model to Investigate Heritability of Changes in Cortical Thickness

The phenotypic measurements of cortical thickness at the three ages were used to define a longitudinal twin model at every vertex of the brain surface model (Fig. 1). From this longitudinal model, we obtained estimates for heritability of changes in cortical thickness; i.e., genetic factors influencing the rate of cortical thinning during childhood and adolescence. Subsequently, we attempt to identify if heritability of changes in cortical thickness are due to increasing (i.e., amplification) or decreasing (i.e., deamplification) influences of the same genetic factor influencing cortical thickness at both ages, or if heritability of changes in cortical thickness is due to the emergence of a novel genetic factor unique for the second age (i.e., genetic innovation; Fig. 2). Genetic innovation can also represent the disappearance of a genetic factor unique for the first age, which unfortunately is indistinguishable in the current model due to symmetry. Derivation for the estimation of heritability of changes in cortical thickness are as follows. For simplification of the mathematical equations, we will refer to the measurement at age 9 years as wave 1, refer to the measurement at age 12 years as wave 2, and refer to the measurement at age 17 years as wave 3. Phenotypic variance of change $V_{\Delta_{ij}}$ in cortical thickness between wave i and wave j can be derived from the phenotypic variance matrix V of the cortical thickness measures as the sum of the phenotypic variance at the individual waves reduced by twice the phenotypic covariance between the two waves. The same rule applies to genetic $A_{\Delta_{ij}}$ and environmental $E_{\Delta_{ij}}$ variance of changes in cortical thickness. For example, the genetic variance of changes $A_{\Delta_{ij}}$ in cortical thickness between wave $i = 1$ and wave $j = 2$ is defined as

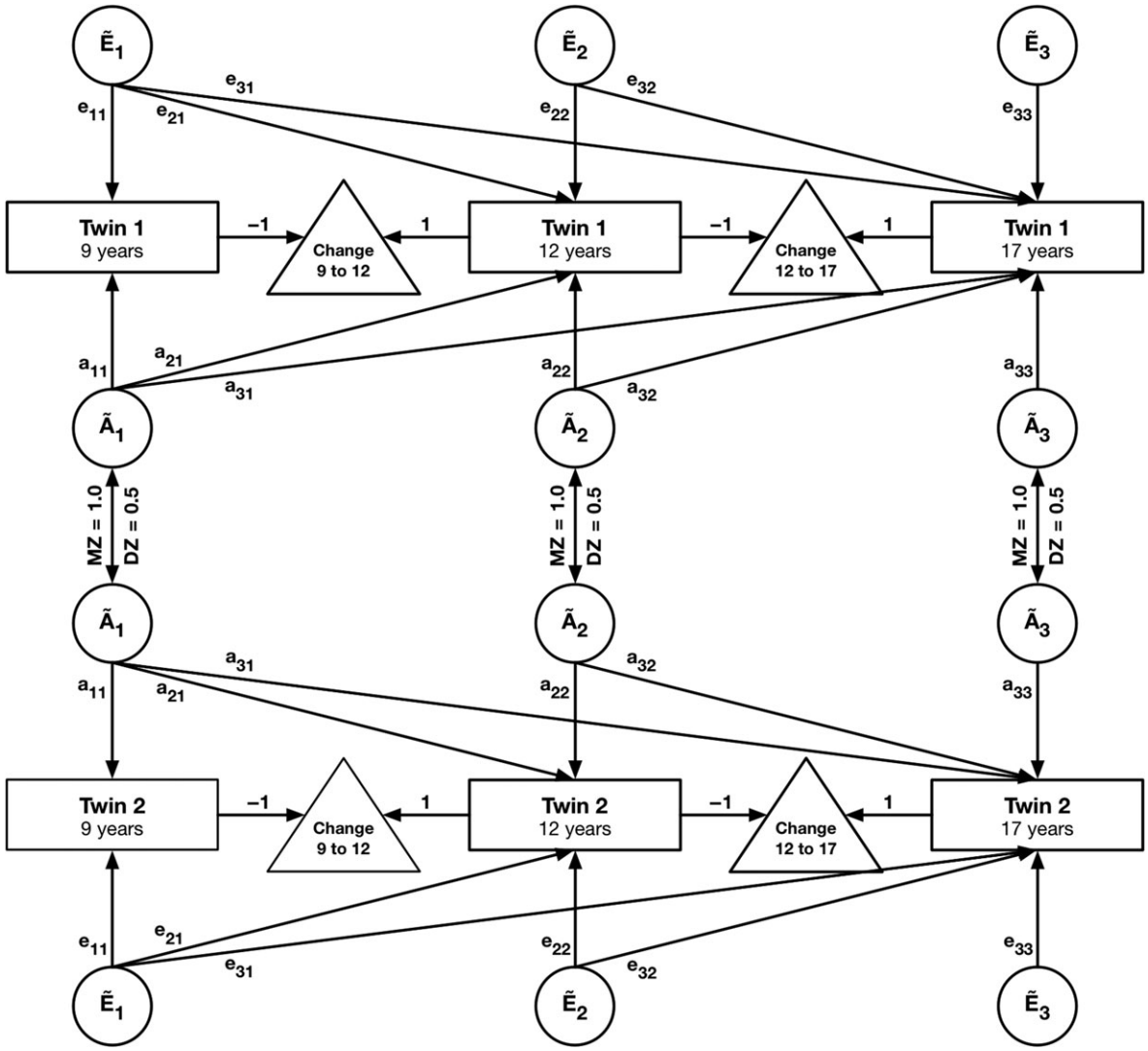

Figure 1. Path diagram of longitudinal AE model used to determine the heritability of changes in cortical thickness. The longitudinal cortical thickness measurements for a region of interest at age 9, 12, and 17 years are used as observed variable (rectangular boxes) for the first (upper half of path diagram) and the second twin (lower half of the path diagram) of each twin pair. Change rates in cortical thickness (triangles) are computed by the model as the difference between the observed variables Independent genetic factors $\tilde{A}_1$, $\tilde{A}_2$, and $\tilde{A}_3$ (circles) load onto the longitudinal cortical thickness measurements through path coefficients. The genetic factor $\tilde{A}_1$ represents genetic influences shared across all three ages through path coefficients a_{11}, a_{21}, and a_{31}. The genetic factor $\tilde{A}_2$ represents genetic influences shared only between age 12 and 17 years through path coefficients a_{22} and a_{32}. The genetic factor $\tilde{A}_3$ represents genetic influences specific for age 17 years through path coefficients a_{33}. The same motif applies for the unique environmental factors $\tilde{E}_1$, $\tilde{E}_2$ and $\tilde{E}_3$, and path coefficients e_{11}, e_{21}, e_{31}, e_{22}, e_{32}, e_{33}. The model is made identifiable by constraining the correlation between genetic factors of both twins to 1.0 in case of monozygotic twins and 0.5 in case of dizygotic twins.

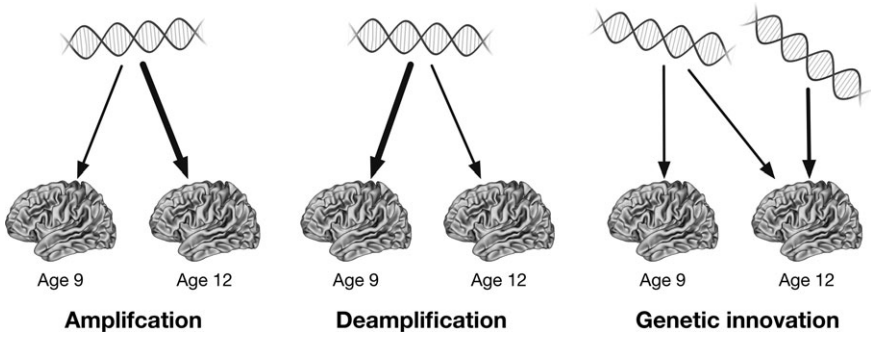

Figure 2. Schematic depiction of genetic amplification, deamplification, and innovation in an example with two ages. For genetic (de)amplification, the same genetic factor influences the phenotype during both ages, but to a greater extent during the second age compared with the first age for genetic amplification, and to a lesser extent during the second age compared with the first age for genetic deamplification. For genetic innovation, the same genetic factor may influence the phenotype during both ages, and an additional genetic factor that is distinct from the first genetic factor and unique to the second age influences the phenotype during the second age.

$$A_{\Delta_{12}} = A_{11} + A_{22} - 2 \cdot A_{12}$$

and the genetic variance of changes $A_{\Delta_{ij}}$ in cortical thickness between wave $i = 2$ and wave $j = 3$ is defined as

$$A_{\Delta_{23}} = A_{22} + A_{33} - 2 \cdot A_{23}$$

where A_{ij} is the genetic (co)variance in cortical thickness between wave i and wave j. Heritability of changes ($h^2_{\Delta_{ij}}$) in cortical thickness between wave i and wave j is then the proportion of phenotypic variance of changes $V_{\Delta_{ij}}$ in cortical thickness between wave i and wave j due to additive genetic variance of changes $A_{\Delta_{ij}}$ in cortical thickness between wave i and wave j: $h^2_{\Delta_{12}} = A_{\Delta_{12}}/V_{\Delta_{12}}$ and $h^2_{\Delta_{23}} = A_{\Delta_{23}}/V_{\Delta_{23}}$

Using a similar rationale as in van Soelen et al. (2012b), genetic variance of changes in cortical thickness between wave 1 and 2 (i.e., $A_{\Delta_{12}}$) can be calculated as $a^2_{11} + a^2_{22} + a^2_{21} - 2 \cdot (a_{21} \cdot a_{11})$ using path tracing rules; simplified, this gives $A_{\Delta_{12}} = a^2_{22} + (a_{11} - a_{21})^2$ (see Fig. 1 for definition of the path coefficients a_{ij}). The first part of the equation represents the contribution of genetic factor $\tilde{A}_2$ specific for wave 2, while the second part represents gradual changes in influences of genetic factor $\tilde{A}_1$ on cortical thickness from wave 1 to wave 2. When $a_{22} > 0$ we speak of genetic innovation at wave 2. When $a_{21} > a_{11}$ we speak of genetic amplification of factor $\tilde{A}_1$ between wave 1 and wave 2, and when $a_{21} < a_{11}$ we speak of genetic deamplification of factor $\tilde{A}_1$ between wave 1 and wave 2. Using the same path tracing approach, genetic variance of change between wave 2 and 3 (i.e., $A_{\Delta_{23}}$) is calculated as $a^2_{22} + a^2_{21} + a^2_{33} + a^2_{32} + a^2_{31} - 2 \cdot (a_{31} \cdot a_{21} + a_{32} \cdot a_{22})$; simplified, this gives $A_{\Delta_{23}} = a^2_{33} + (a_{22} - a_{32})^2 + (a_{21} - a_{31})^2$ (see Fig. 1 for definition of the path coefficients a_{ij}). The first part of the equation represents the contribution of genetic factor $\tilde{A}_3$ specific for wave 3, the second part represents gradual changes in influences of genetic factor $\tilde{A}_2$ on cortical thickness from wave 2 to wave 3, and the third and last part represents gradual changes in influence of genetic factor $\tilde{A}_1$ on cortical thickness from wave 2 to wave 3. When $a_{33} > 0$ we speak of genetic innovation at wave 3. When $a_{31} > a_{21}$ we speak of genetic amplification of factor $\tilde{A}_1$ between wave 2 and wave 3, and when $a_{31} < a_{21}$ we speak of genetic deamplification of factor $\tilde{A}_1$ between wave 2 and wave 3. When $a_{32} > a_{22}$ we speak of genetic amplification of factor $\tilde{A}_2$ between wave 2 and wave 3, and when $a_{32} < a_{22}$ we speak of genetic deamplification of factor $\tilde{A}_2$ between wave 2 and wave 3.

Determining the Source of Heritability of Changes in Cortical Thickness

Heritability of changes in cortical thickness can be the result of innovation of novel genetic factors or (de)amplification of existing genetic factors. We employed a step-wise nested model testing approach to determine the most likely origin of the heritability of changes in cortical thickness. First, we determined all vertices that show significant heritability of changes in cortical thickness (FDR adjusted $q < 0.05$; Genovese et al. 2002) between wave 1 and 2 and similarly between wave 2 and 3. For those vertices, we first tested whether the heritability of changes in cortical thickness originated from innovation of genetic factors. Testing for innovation of genetic factor $\tilde{A}_2$ at wave 2 was performed by comparing the model with path coefficient a_{22} and a_{32} constrained to zero to the base model without any constraints. Testing for innovation of genetic factor $\tilde{A}_3$ at wave 3 was performed by comparing the model with path coefficient a_{33} constrained to zero to the base model without any constraints.

If no evidence for innovation was found, we continued with testing for (de)amplification of existing genetic factors. All models testing for (de)amplification of existing genetic factors were compared with a reference model where no innovation of genetic factors was possible by constraining path coefficients a_{22}, a_{32}, and a_{33} to zero. Testing for (de)amplification of genetic factor $\tilde{A}_1$ between wave 1 and 2 was performed by additionally constraining path coefficient a_{11} to be equal to a_{21} in the model and comparing it to the reference model. Testing for (de)amplification of genetic factor $\tilde{A}_1$ between wave 2 and wave 3 was performed in the same way by additionally constraining path coefficient a_{21} to be equal to a_{31} instead.

Statistical Significance of Parameters

Statistical significance of heritability of cortical thickness (and heritability of changes in cortical thickness) was tested comparing the –2 log-likelihood of the unconstrained model to the –2 log-likelihood of the nested model with the heritability estimate at a given age (or interval) constrained to a fixed value of 0. This statistic asymptotically follows a 50:50 mixture of χ^2 distributions with zero and one degree of freedom; allowing P-values to be cut in half (Dominicus et al. 2006). Likewise, statistical significance of differences in heritability of cortical thickness between ages was determined by comparing the unconstrained model and a nested model in which the heritability estimates at the different ages were set to be equal.

Bivariate Twin Model to Investigate Overlap in Genetic and Environmental Factors Between Brain Regions

To investigate the presence of interrelationship in genetic and environmental factors between two brain regions across space *and* age, we estimated the genetic and environmental correlation for all possible pairs of regions of interest across the 3 waves. The genetic correlation (r_g) between region x at wave i and region y at wave j is defined as

$$r_g(x_i, y_j) = \frac{A_{x_i y_j}}{\sqrt{A_{x_i} A_{y_j}}}$$

where $A_{x_i y_j}$ is the genetic covariance between the two regions, and A_{x_i} and A_{y_j} represent the genetic variance of the individual regions. The same definition applies to environmental correlation (r_e) using environmental (co)variances $E_{x_i y_j}$, E_{x_i} and E_{y_j}. Sequential bivariate analysis of all 630 unique pairwise bivariate models (6 lobar regions per hemisphere for each wave) was employed to populate a unitriangular matrix with dimensions 36 × 36 cells for the phenotypic (r_{ph}), genetic (r_g) and environmental (r_e) correlation between regions of interest; a path diagram of the bivariate AE model used in the analysis is presented in Supplementary Fig. S2. Statistical significance of a correlation was tested using a χ^2 distribution with one degree of freedom on the difference in log-likelihood of the unconstrained model and a nested model with the correlation constrained to a fixed value of −1, 0, or +1. Correlation matrices were visualized using the *corrplot* package in R (Wei and Simko 2016). Next, we applied cluster analysis to the separate phenotypic and genetic correlation matrices to extract groups of regions with high phenotypic, genetic, or environmental similarity.

Cluster Analysis Based on Phenotypic, Genotypic, and Environmental Correlation Matrices

To investigate spatial and temporal patterns of the cortex we applied a hierarchical clustering algorithm to the phenotypic, genetic, and environmental correlation matrices obtained from the bivariate twin model using the *cluster* package in R (Maechler et al. 2016). Prior to clustering, the phenotypic and genetic correlation matrices were transformed into dissimilarity matrices using $1 - r_{ph}$ for the phenotypic correlation matrix, $1 - |r_g|$ for the genotypic correlation matrix, and $1 - |r_e|$ for the environmental correlation matrix. For the phenotypic correlation matrix, this transformation ensured that highly correlated regions would have low dissimilarity whereas anticorrelated regions would have high dissimilarity. In contrast, for the genotypic and environmental correlation matrices, both highly correlated and anticorrelated regions (i.e., regions under the influence of the same genes or environmental factors but with opposing effects on the phenotype) would have low dissimilarity. The optimal number of clusters k_{opt} was determined by selecting the minimum value of k for which the average silhouette width was within one standard error of the maximum average silhouette width (Rousseeuw 1987).

Post-hoc Analyses

To investigate the possible effects of confounds on the results of the analyses, we performed a qualitative post-hoc analysis using twin models where cortical thickness measurements were corrected for sex, age at scan (and thereby implicitly individual scan interval between ages), and handedness. Residuals after linear regression of covariates on the cortical thickness data were used as input to the structural equation models. We performed a qualitative evaluation of the effects of confounds by visual inspection of the cortical maps and correlation matrices with and without regression of covariates.

Since heteroscedasticity between groups can have greater influences on the results in twin modeling than correcting for mean effects, we performed a quantitative post-hoc analysis to investigate the effects of sex and handedness on the mean and variance of whole-brain cortical thickness estimates. We used a univariate saturated twin model with coefficients on the mean and (co)variance estimates to model effects of sex and handedness. The statistical significance of the effects was tested using a χ^2 distribution with one degree of freedom on the difference in log-likelihood of the unconstrained model and a nested model with the coefficient constrained to a fixed value of 0.

Results

Development of Cortical Thickness

The mean global cortical thickness was 3.38, 3.31, and 3.07 mm at age 9, 12, and 17 years (Fig. 3*a*; Supplementary Table S3). A quadratic age curvature best described the trajectory of cortical thickness development (cubic vs. quadratic: $p = 0.7863$); (quadratic vs. linear: $p < 0.001$). The linear approximation of the annual rate of change between the ages 9 and 12 years was –0.023 mm/year (CI_{95} [–0.028 to –0.018 mm/year]; $p < 0.001$) and doubled to –0.049 mm/year (CI_{95} [–0.052 to –0.045 mm/year]; $p < 0.001$) between the ages 12 and 17 years (Fig. 3*a*; Supplementary Table S3). No significant effects of sex ($p > 0.302$) or handedness ($p > 0.243$) on mean global cortical thickness or changes in mean global cortical thickness (sex: $p > 0.081$; handedness: $p > 0.145$) were found (Fig. 3*a*). No significant effects of sex ($p > 0.469$) or handedness ($p > 0.107$) on variance of mean global cortical thickness or changes in mean global cortical thickness (sex: $p > 0.060$; handedness: $p > 0.305$) were found.

As previously reported (van Soelen et al. 2012b), at age 9 years, regions with highest cortical thickness are found at the insula, temporal pole, and medial frontal areas, with local thickness up to 4.58 mm (Fig. 3*b*; Supplementary Video S1). Regions with lowest cortical thickness are found in the visual cortex and sensorimotor cortices, with local thickness down to 2.81 mm (Fig. 3*b*; Supplementary Video S1). Between the ages 9 and 12 years there is a subtle decrease in cortical thickness for most parts of the cortex, whereas some parts of the cortex, such as the bilateral gyrus rectus, parahippocampal gyrus, and superior- and middle temporal poles, show nonsignificant changes in cortical thickness (Fig. 3*c*). The decrease in cortical thickness is most prominent at the visual cortex, primary sensory and motor cortices, and frontal poles, with rate of change between –0.03 and –0.05 mm/year (Fig. 3*c*).

When including the third measurement at age 17 years, we found that the rate of changes in cortical thickness between the ages 12 and 17 years accelerates and expands to most regions of the cortex, with local maximum rate of change reaching up to –0.16 mm/year in the superior frontal gyrus (Fig. 3*c*). The least decrease in cortical thickness occurs bilaterally at parahippocampal gyrus, olfactory cortex, and cingulum, with rate of change between 0.01 to 0.02 mm/year (Fig. 3*c*).

Heritability of Cortical Thickness

Heritability of mean global cortical thickness was 62% (CI_{95} [46–74%]; $p < 0.001$) at age 9, 80% (CI_{95} [65–88%]; $p < 0.001$) at

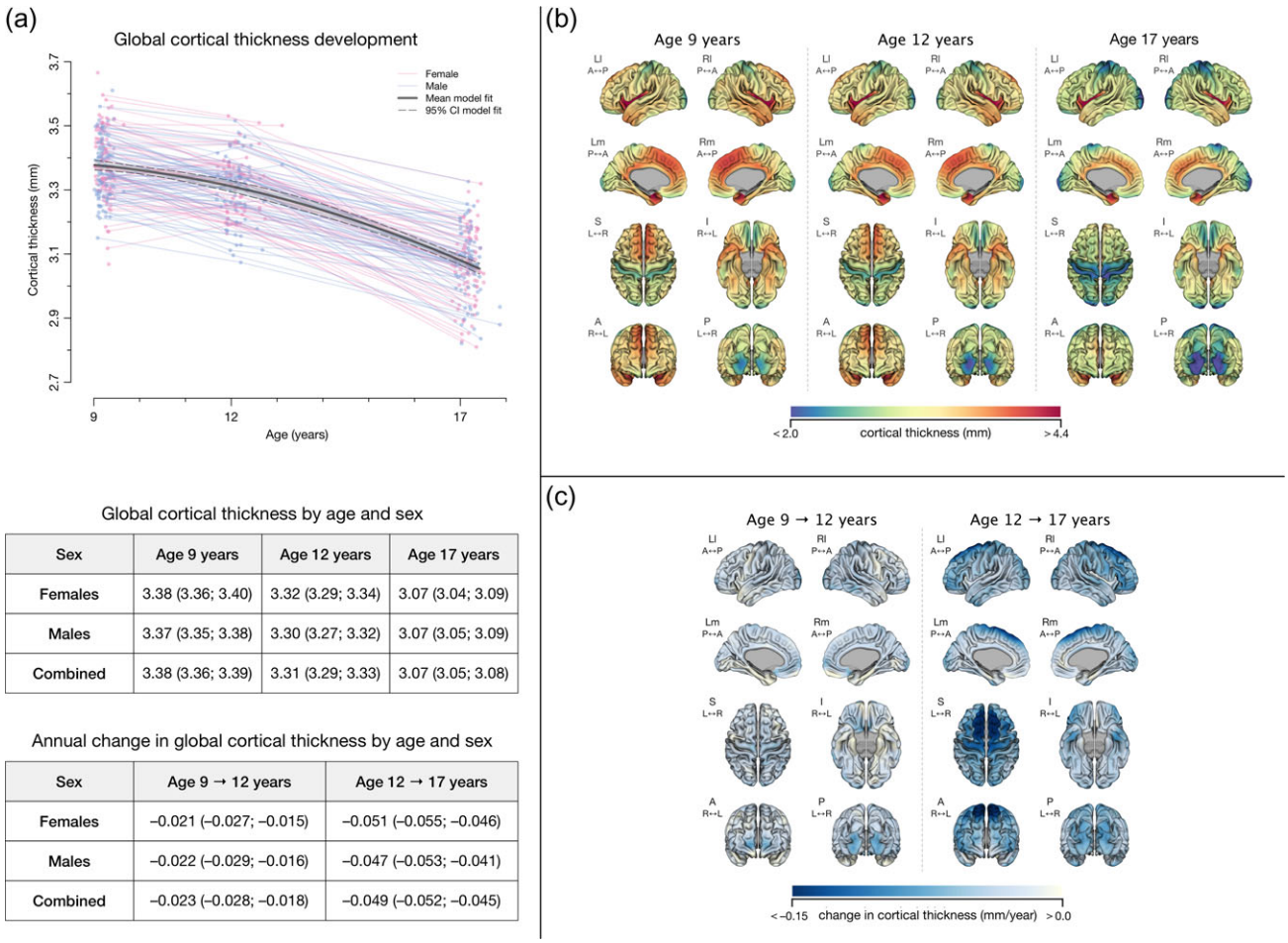

Global cortical thickness by age and sex

Sex	Age 9 years	Age 12 years	Age 17 years
Females	3.38 (3.36; 3.40)	3.32 (3.29; 3.34)	3.07 (3.04; 3.09)
Males	3.37 (3.35; 3.38)	3.30 (3.27; 3.32)	3.07 (3.05; 3.09)
Combined	3.38 (3.36; 3.39)	3.31 (3.29; 3.33)	3.07 (3.05; 3.08)

Annual change in global cortical thickness by age and sex

Sex	Age 9 → 12 years	Age 12 → 17 years
Females	−0.021 (−0.027; −0.015)	−0.051 (−0.055; −0.046)
Males	−0.022 (−0.029; −0.016)	−0.047 (−0.053; −0.041)
Combined	−0.023 (−0.028; −0.018)	−0.049 (−0.052; −0.045)

Figure 3. Developmental pattern of (*a*) global and (*b*,*c*) local cortical thickness during childhood and adolescence. (*a*) Global cortical thickness shows accelerated thinning during adolescence. Data points represent individual measurements, with lines connecting data points representing longitudinal measurements between age 9 and 12 years, and between age 12 and 17 years. A quadratic model best described overall thinning of mean global cortical thickness (thick solid line accompanied by 95% confidence interval). No significant sex effects were found for global cortical thickness at any age nor for annual change rates in global cortical thickness at either scan intervals. Values reported in tables are mean and 95% confidence interval. (*b*) Absolute cortical thickness across the ages 9 years (left panel), 12 years (middle panel), and 17 years (right panel) reveal regional effects of cortical thinning during adolescence. Cortical thickness ranges from less than 2.0 mm (blue) in the occipital cortex at age 17 years up to greater than 4.4 mm (red) in the insular cortex at age 9 years. (*c*) Annual development of cortical thickness between ages 9 and 12 years (left panel), and between ages 12 and 17 years (right panel) based on linear approximation emphasize regional differences in rate of cortical thinning, particularly in the medial frontal cortex. The rate of changes in cortical thickness ranges from nonsignificant changes in cortical thickness per year (white) in mostly medial temporal regions between age 9 and 12 years to a decrease in cortical thickness of 0.15 mm/year or greater (dark blue) in medial frontal cortex between age 12 and 17 years. The rate of cortical thinning doubles between the ages 12 and 17 years compared with the rate of change between the ages 9 and 12 years. (*b*,*c*) Order of views per age, from left to right, top to bottom: left lateral (Ll), right lateral (Rl), left medial (Lm), right medial (Rm), superior (S), inferior (I), anterior (A), and posterior (P).

age 12, and 54% (CI_{95} [32–70%]; $p < 0.001$) at age 17 years; see Supplementary Fig. S3 for local heritability estimates of cortical thickness and Supplementary Table S3 for regional heritability estimates. Differences in heritability of mean global cortical thickness was significant between ages 12 and 17 years ($p = 0.036$), but not significant between ages 9 and 12 years ($p = 0.104$ [n.s.]) or between ages 9 and 17 years ($p = 0.495$ [n.s.]).

Hierarchical Clustering of Phenotypic and Genetic Correlation Matrices

A highly correlated genetic factor was involved in mean global cortical thickness at ages 9 and 12 years (r_g=0.92; CI_{95} [0.75–1.00]). While there was significant genetic overlap between age 9 and age 17 years (r_g=0.68; CI_{95} [0.40–0.94]) and age 12 and age 17 years (r_g=0.64; CI_{95} [0.41–0.87]), the confidence intervals of the genetic correlations suggest additional genetic factors influencing cortical thickness at age 17 years.

We estimated the phenotypic, genetic, and environmental correlations of cortical thickness between the major lobes of the cortex across childhood and adolescent development (Fig. 4). The phenotypic and environmental correlation matrices show strong similarities in pattern. There is a moderate to strong association between the major lobes within hemisphere (Fig. 4*a*,*c*), and a strong association between homologous regions across hemispheres within each age for phenotypic correlations that is absent for environmental correlations (Fig. 4*a*,*c*). In addition, both phenotypic and environmental correlations show an association of the same regions over time, although this association is only weak to moderate for environmental correlations (Fig. 4*a*,*c*). In contrast, genotypic correlations show strong association between all regions across all three ages. However, many of the association with regions at age 17 years are absent due to nonsignificant

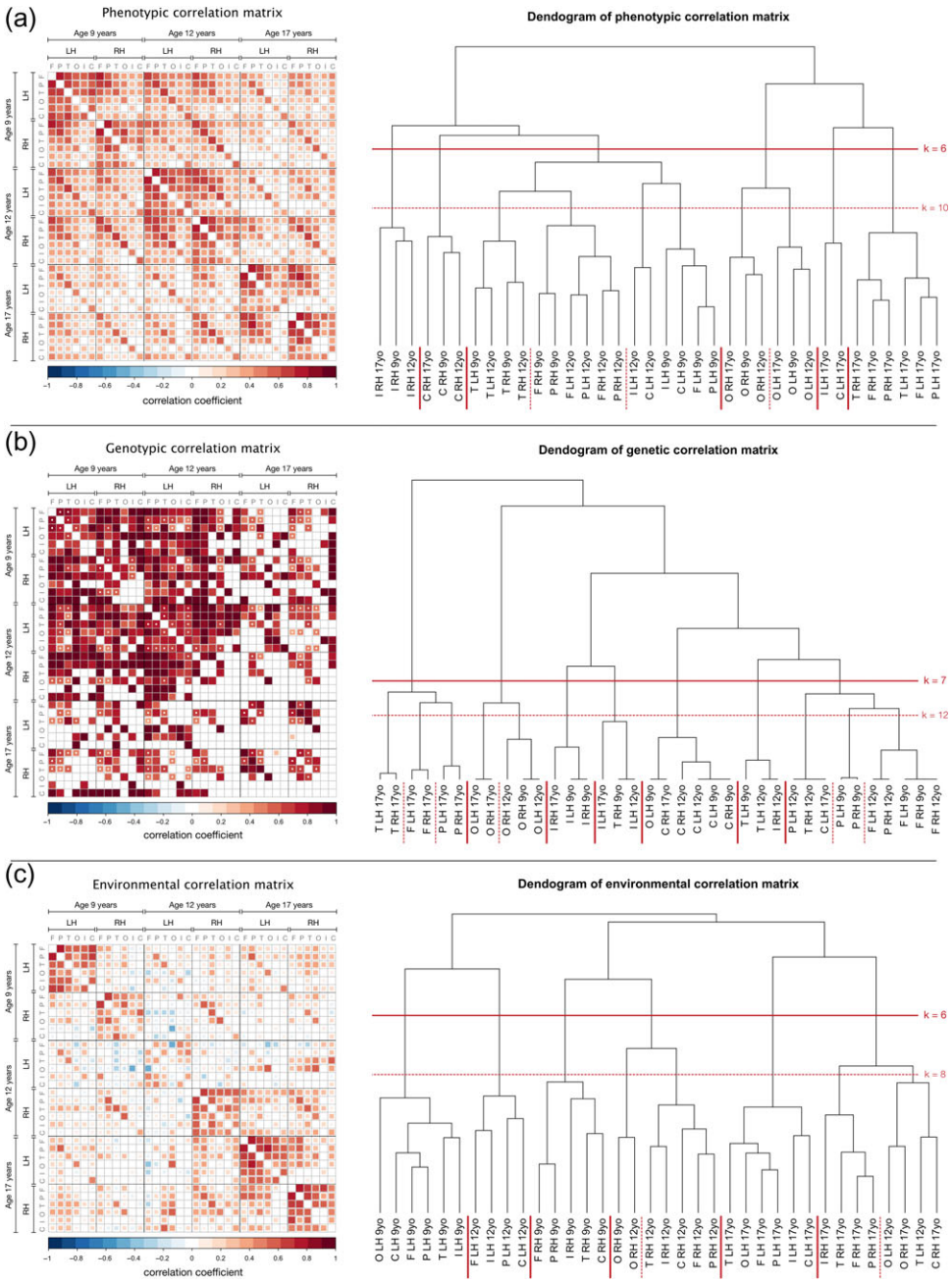

Figure 4. Hierarchical clustering of the phenotypic, genetic, and environmental correlation matrix of absolute cortical thickness across childhood and adolescent development. (*a*) The correlation matrices for phenotypic (top), genetic (middle), and environmental (bottom) correlation in cortical thickness between the major lobes of the cortex. Correlations range from −1 (blue) to +1 (red). Correlations that did not differ from zero ($p > 0.05$; uncorrected) are left blank. Genetic correlations marked with a white dot indicate incomplete pleiotropy (i.e., unique genetic factors for each region in addition to a shared genetic factor). Regions are ordered from top-left to bottom-right, first by age (9, 12, and 17 years), then by hemisphere (LH = left hemisphere, and RH=right hemisphere), and finally by lobe (F=frontal, P=parietal, T=temporal, O=occipital, I=insula, and C=cingulate). (*b*) Dendrogram for the hierarchical clustering of the distance-transformed phenotypic (top), genotypic (middle), and environmental (bottom) correlation matrices. Phenotypic correlations were transformed using one minus the phenotypic correlation, and genetic and environmental correlations were transformed using one minus the absolute of the genetic or environmental correlation. The optimal number of clusters was determined by the average silhouette (see Supplementary Fig. S4); k_{opt}=6 for the phenotypic correlation matrix, k_{opt}=7 for the genetic correlation matrix, and k_{opt}=6 for the environmental correlation matrix. Optimal clusters are separated by a solid red line, while global optimum uses a dotted red line. Labels for the regions are encoded as lobe (F=frontal, P=parietal, T=temporal, O=occipital, I=insula, and C=cingulate), followed by hemisphere (LH=left hemisphere, and RH=right hemisphere), and finally age (9yo=age 9 years, 12yo=age 12 years, and 17yo=age 17 years).

associations (Fig. 4*b*). Although many regions share a common genetic factor, a portion of these regions are influenced by an additional genetic factor unique for each region (i.e., incomplete pleiotropy), indicated by a white dot (Fig. 4*b*). Of special note, regions within the same age are influenced by distinct genetic factors (i.e., spatial genetic differentiation of lobes), as well as the same regions across age (i.e., temporal genetic differentiation): left parietal cortex and right frontal cortex between age 9 and 17 years, and right parietal between age 12 and 17 years.

We performed hierarchical clustering analysis on the correlation matrices (Fig. 4). The optimal number of clusters k_{opt} was determined using the silhouette heuristic (Rousseeuw 1987); k_{opt}=6 for the phenotypic correlation matrix, k_{opt}=7 for the genetic correlation matrix, and k_{opt}=6 for the environmental correlation matrix (Supplementary Fig. S4). The global pattern reveals the insular cortex and cingulate cortex form separate clusters from the frontal, temporal, and parietal lobes, with occipital lobe forming a third independent cluster. Clustering of the phenotypic and genetic correlation matrices separates the frontal, parietal, and temporal lobes at age 17 years from age 9 and 12 years (Fig. 4*a*,*b*). In addition, clustering of the genetic correlation matrix pairs homotopic regions across hemisphere, whereas clustering of phenotypic correlation matrix regions groups regions by hemisphere (Fig. 4*a*,*b*). In contract, clustering of the environmental correlation matrix reveals a strong pattern where regions are first clustered by age followed by hemisphere (Fig. 4*c*). The described patterns become more apparent when using regions from only one or two of the ages (Supplementary Fig. S5).

Post-hoc analysis on the effects of possible confounds revealed little effect from sex, age at scan, and handedness on the correlation matrices of cortical thickness between cerebral lobes (Supplementary Fig. S6).

Heritability of changes in cortical thickness

Heritability of changes in mean global cortical thickness is 21% (CI_{95} [0–52%]; $p = 0.154$ [n.s.]) between the ages 9 and 12 years, and 53% (CI_{95} [26–72%]; $p < 0.001$) between the ages 12 and 17 years; see Supplementary Table S3 for regional heritability of changes in cortical thickness. Locally, heritability of changes in cortical thickness is most prominent at association cortices in the frontal, parietal, and temporal lobes (FDR adjusted $q < 0.05$), where it reaches up to 76% heritability between the ages 9 and 12 years, and up to 82% heritability between the ages 12 and 17 years (Fig. 5*a*).

Post-hoc analysis on the effects of possible confounds reveals little effect from sex, age at scan and handedness on heritability of changes in cortical thickness (Supplementary Fig. S7).

Decomposition of Heritability of Changes in Cortical Thickness

Locally, we find several large clusters of genetic innovation in the right superior medial frontal gyrus, near the right calcarine sulcus, right superior medial frontal gyrus, left medial orbital frontal cortex, right parahippocampal gyrus, left fusiform gyrus, right Heschl gyrus, right middle frontal gyrus, bilateral postcentral gyrus, and right middle occipital gyrus between age 9 and 12 years (Fig. 5*b* and Table 1). These clusters show strong heritability of changes in cortical thickness with estimates between 40% and 71% (FDR adjusted $q < 0.023$) and genetic innovation ($p < 0.017$). Between age 12 and 17 years, large clusters of genetic innovation were found at the right superior medial frontal cortex, right lingual gyrus, left supramarginal gyrus, left calcarine sulcus, and left superior parietal gyrus (Fig. 5*b* and Table 1). These clusters show similarly strong heritability of changes in cortical thickness with estimates between 50% and 70% (FDR adjusted $q < 0.024$) and genetic innovation ($p < 0.017$).

In addition to genetic innovation, we found clusters of genetic (de)amplification becoming more widespread throughout the cortex during later adolescence, with most evident amplification in the right supramarginal gyrus, and deamplification in the medial frontal cortex, cingulum, and occipital cortex between the ages 12 and 17 years (Fig. 5*b*).

Post-hoc analysis on the effects of possible confounds revealed little effect from sex, age at scan and handedness on the decomposition of heritability of changes in cortical thickness (Supplementary Fig. S7).

Discussion

We applied twin modeling to a longitudinal cohort with 3 measurements to investigate the extent to which genetic influences drive *changes in cortical thickness* during childhood and adolescence. We find a single genetic factor that affects the acceleration of overall cortical thinning across childhood and adolescent development with increasing heritability of changes in mean global cortical thickness: $h^2_{\Delta 12}$=21% ($p = 0.154$; [n.s.]) between ages 9 and 12 years, and $h^2_{\Delta 23}$=53% ($p < 0.001$) between ages 12 and 17 years. At age 17 years, a new genetic factor comes in to play, separating cortical thickness development in late adolescence from early adolescence and childhood. Locally, we again find a core genetic factor influencing cortical thickness and a second genetic factor involved in innovation explaining changes in local cortical thickness during different stages of childhood and adolescent development; areas with the highest estimates include the anterior cingulate cortex (h^2=71% in cortical thickness change between age 9 and 12 years) and the superior medial frontal cortex (h^2=70% in cortical thickness change between age 12 and 17 years).

We report an accelerating decrease in cortical thickness in twins in this longitudinal design with up to 3 measurements (Fig. 3; Supplementary Table S3) that is compatible with cortical development in healthy typically developing singletons (Gogtay et al. 2004; Sowell et al. 2007; Raznahan et al. 2011b; Storsve et al. 2014; Schnack et al. 2015). The patterns in phenotypic correlation across time (Fig. 4*a*), with strong correlations between homotopic regions and correlation of the same region across development, are comparable to those found by structural covariance analyses (Raznahan et al. 2011a; Alexander-Bloch et al. 2013). We find moderate to high heritability estimates of cortical thickness for most of the cortex, corroborating the evidence that the cortex is under strong genetic control (Lenroot et al. 2009; Blokland et al. 2012; Schmitt et al. 2014). Estimating the genetic overlap in cortical thickness between lobar regions of the cortex revealed a strong core genetic factor affecting overall cortical thickness across childhood and adolescent development (Fig. 4*b*). The evidence for a core genetic factor is in agreement with one of the earlier studies investigating distinct genetic influences on cortical thickness in a cross-sectional pediatric sample with age range from 5.4 to 18.7 years that found a single component explaining over 60% of the genetic variance (Schmitt et al. 2008). Another cross-sectional study in older male-only twins found moderate to strong genetic correlations ranging from 0.3 to 1.0 across most of the cortex, characteristic for an omnipresent genetic factor, for a seed placed in the middle frontal cortex (Rimol et al. 2010). We now add to these findings that the same genetic factor is responsible for cortical *thinning* during childhood and adolescence.

In contrast to cross-sectional studies investigating regional genetic influences on cortical thickness *after* removing the effect of global cortical thickness (Schmitt et al. 2008; Eyler et al. 2012; Chen et al. 2013; Docherty et al. 2015; Fjell et al. 2015), we specifically wanted to investigate the temporal

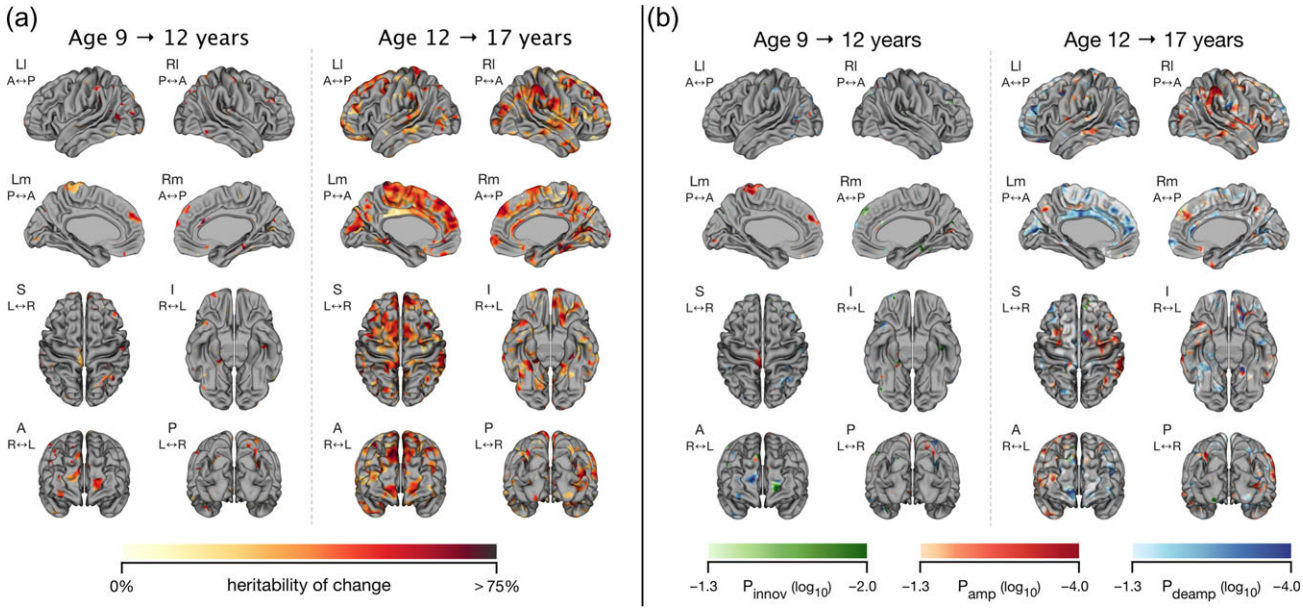

Figure 5. Estimated heritability of (*a*) changes in cortical thickness and (*b*) its decomposition into different genetic origins between the ages 9 and 12 years (left panel), and between the ages 12 and 17 years (right panel). (*a*) Heritability estimates that did not differ significantly from zero (FDR adjusted $q > 0.05$) have been left grey. Approximately 3.1% of the vertices between age 9 and 12 years and 28.4% of the vertices between age 12 and 17 years are significant for heritability of changes in cortical thickness (FDR adjusted $q < 0.05$). Heritability estimates range from 0% (light-yellow) up to 75% or greater (dark-red). (*b*) Heritability of changes in cortical thickness between the ages 9 and 12 years (left panel) and between the ages 12 and 17 years (right panel) was decomposed into sources of genetic innovation (green; 20.2% of the vertices significant for heritability of changes in cortical thickness between the ages 9 and 12 years, and 1.2% between the ages 12 and 17 years), and areas with amplification (red; 49.2% of the vertices between the ages 9 and 12 years, and 29.3% between the ages 12 and 17 years) or deamplification (blue; 28.5% of the vertices between the ages 9 and 12 years, and 28.4% between the ages 12 and 17 years) of a genetic factor across age. Areas with significant heritability of changes in cortical thickness for which these sources could not be disentangled are depicted in light grey (remaining 2.1% of the vertices significant for heritability of changes in cortical thickness between the ages 9 and 12 years, and 41.1% between the ages 12 and 17 years). Scale bars for significance start at $\log_{10}$-equivalent of p=0.05. (*a*, *b*) Order of views per age, from left to right, top to bottom: left lateral (Ll), right lateral (Rl), left medial (Lm), right medial (Rm), superior (S), inferior (I), anterior (A), and posterior (P).

Table 1 Overview of largest clusters with genetic innovation between age 9 and 12 years and between age 12 and 17 years; based on the size distribution of the clusters, only the largest clusters with 10 or more vertices in size are included in this table (approximately top 15% largest clusters), ordered by anatomical position along the anterior–posterior axis

#	Region	Size	MNI coordinates			$h^2(\Delta CT)$	$p(h^2(\Delta CT))$	$p(Innov)$
Age 9–12 years								
1	Med. Orb. Frontal LH	40	−17	69	−2	53%	0.020	0.004
2	Mid. Orb. Frontal RH	10	26	55	−15	48%	0.033	0.003
3	Sup. Med. Frontal RH	43	4	50	41	47%	0.023	0.010
4	Ant. Cingulum RH	12	3	24	22	71%	0.027	0.017
5	Fusiform Gyrus LH	28	−39	−14	−34	54%	0.010	<0.001
6	Heschl Gyrus RH	26	37	−25	12	41%	0.027	0.001
7	Heschl Gyrus LH	10	−35	−29	17	41%	0.036	0.003
8	Parahippocampal RH	38	17	−32	−16	68%	0.013	<0.001
9	Calcarine Sulcus RH	48	15	−65	5	62%	0.013	0.010
10	Cuneus LH	10	−15	−75	37	44%	0.032	0.002
Age 12–17 years								
1	Sup. Med. Frontal RH	55	11	53	5	70%	0.003	0.013
2	Sup. Med. Frontal RH	53	7	44	41	66%	0.004	0.018
3	Calcarine Sulcus LH	11	−19	−46	−34	52%	0.025	0.004
4	Lingual Gyrus RH	39	14	−60	−2	67%	0.002	0.006
5	Sup. Parietal LH	10	−4	−71	12	57%	0.011	0.015
6	Supramarginal Gyrus LH	22	−18	−102	−16	50%	0.007	0.016

Region are defined by the Automated Anatomic Labeling (AAL) Atlas (Tzourio-Mazoyer et al. 2002); size is reported as the number of connected vertices in the cluster; MNI coordinates are reported in XYZ format; $h^2(\Delta CT)$ = heritability of changes in cortical thickness; $p(h^2(\Delta CT))$ = significance of heritability of changes in cortical thickness (FDR adjusted $q<0.05$); $p(Innov)$ = significance of genetic innovation (uncorrected $p<0.05$).

dynamics of the genetic factor affecting overall cortical thickness development during childhood and adolescence. Using the longitudinal twin model setup, we show there is a single genetic factor that dominates across childhood and adolescence which is involved in cortical thickness *and* cortical thickness change—and thus involved in cortical thinning. On top of

this core genetic factor there is evidence for spatial genetic differentiation between the major lobes. This corroborates results from a recent publication in an extended longitudinal twin design that finds similar spatial patterns for genetic correlations of cortical thickness between the major lobes during childhood and adolescence (Schmitt et al. 2017). In addition, they show changes in genetic correlation across development, with some regions demonstrating an increase in genetic overlap towards the second decade of life. Their results could be related to the fluctuating influences of genes and genetic innovation found in our study and is characteristic for genetic differentiation. This genetic differentiation might be the result of continued areal specialization of the cortex, since it is well known that cortical areas continue to develop well into early adulthood and beyond, in particular the frontal cortex (Schnack et al. 2015). During adolescence, areal specialization might be spurred by new genetic factors that could be related to the rapid cognitive and behavioral changes during adolescence.

Indeed, decomposition of genetic influences on cortical plasticity revealed a second genetic factor, representing genetic innovation, that is influencing cortical thickness during childhood and adolescent development. The areas where genetic innovation occurred were most prominent in the frontal cortex, involving the anterior cingulate cortex (with a heritability of changes in cortical thickness of 71% between age 9 and 12 years) and superior medial frontal cortex (heritability of 70% between age 12 and 17 years). In addition, genetic innovation was found in other areas, such as the medial and middle orbital frontal cortices, the fusiform, Heschl's, and parahippocampal gyri and the cuneus between age 9 and 12 years and the calcarine, lingual, superior parietal and supramarginal cortices between age 12 and 17 years. Together, the two genetic factors involved in changes in cortical thickness explain the strong positive correlations between homotopic regions across the hemispheres and across age, evident from the diagonal banding in the correlation matrices (Fig. 4) and as reported from cross-sectional twin studies at both lobar and local level (Chen et al. 2013; Wen et al. 2016).

Gene expression studies can reveal the spatiotemporal dynamics of individual genes expressed in the human brain across the lifespan (Naumova et al. 2013; Akbarian et al. 2015; Silbereis et al. 2016). It has been suggested that areal specialization of the neocortex is established during early development, and that later development is the result of more general maturational processes affecting the entire neocortex (Pletikos et al. 2014). Several studies report a remarkable homogeneity in gene expression profiles among neocortical areas despite their functional specialization (Roth et al. 2006; Kang et al. 2011; Hawrylycz et al. 2015; Jaffe et al. 2015). Results from our analysis show a similar strong overlap in genetic factors among neocortical areas while providing evidence for spatial differentiation among the major lobes. These results suggest that cortical thickness during childhood and adolescence is primarily driven by a core genetic component with secondary regional-specific genetic influences. This result is in agreement with other twin studies that found distinct regional genetic influences on cortical thickness after removing global effects (Schmitt et al. 2008; Chen et al. 2013; Docherty et al. 2015). It suggests a majority of cortical thinning during childhood and adolescence might be part of a more generic developmental process affecting global cortical development (Jaffe et al. 2015), whereas secondary influences might be the result of gene-environment interactions.

Regarding temporal differential gene expression (i.e., increased or reduced expression of the same genes, or expression of novel genes over time), adolescence is a period during postnatal human development marked by the highest number of temporal differential expression of genes in the prefrontal cortex (Jaffe et al. 2015). During postnatal development, an hourglass model for spatially differential gene expression has been reported, where adolescence is identified by increased homogeneity in spatial gene expression among neocortical areas that is concluded by a second wave of changes in gene expression at the end of adolescence (Somel et al. 2010; Colantuoni et al. 2011; Pletikos et al. 2014). A similar conclusion can be made from our results where age 12 years shows increased complete genetic overlap between cortical regions compared with age 9 and 17 years, although this conclusion should be treated with caution as it might be the result of diminished statistical power to detect genetic differentiation due to reduced sample size at age 12 years. The more pronounced genetic (de)amplification and genetic innovation found in our analysis between age 12 and 17 years might be the first sign of the reported second wave of changes in gene expression at the end of adolescence. Thinning of the cortex during adolescence and early adulthood has been linked to increased myelination and associated gene expression (Whitaker et al. 2016). Gene co-expression network analyses have revealed modules enriched for genes associated with synaptic function, dendrite development and myelination emerging during late fetal development and reaching a plateau during early childhood (Kang et al. 2011). Spatiotemporal differentiation in gene expression profiles have been linked to differences in cellular composition of the neuropil rather than changes in gene expression of constituent cells (Jaffe et al. 2015). These gene expression findings support existing theories on the biological processes underlying the apparent cortical thinning observed during development (Huttenlocher 1979; Bourgeois and Rakic 1993; Huttenlocher and Dabholkar 1997; Paus et al. 2008; Paus 2010; Petanjek et al. 2011; Miller et al. 2012; Deoni et al. 2015). These theories anticipate a decrease in cortical grey matter content of the neuropil due to pruning of neuronal synapses and dendrites accompanied by a decrease in supporting glial cells, and a parallel increase of oligodendrocytes responsible for myelination of neuronal axons. The fluctuating influences of the core genetic factor from our results could represent a shift in balance of maturational processes. Another possible explanation of the fluctuating influences of the core genetic factor could be related to maturational timing of neocortical areas. Neocortical areas that mature during childhood and early adolescence might experience increased influences of a genetic factor associated with maturational genes around that age, followed by a decreased influence upon maturation during later adolescence. In contrast, neocortical areas that mature during late adolescence might initially experience a low or decreased influence of this genetic factor that suppresses or delays maturation until late adolescence. The genetic innovation found in our analysis could represent a novel genetic factor that arises upon maturation of neocortical, such as genes involved in maintain matured neurons in good condition. On the other hand, the genetic innovation could also represent the disappearance of a genetic factor, something we cannot resolve with the current twin model design. This would mean the genetic "innovation" could be associated with the termination of maturational processes instead.

The brain is highly plastic and capable of adapting to new environments (Kramer et al. 2004; Zatorre et al. 2012). The environmental correlations estimated from our data could be due to true environmental influences unique to each individual, but are likely to be confounded by measurement errors from the MRI scans and image processing procedure. In particular, the strong correlations within ages will be confounded by measurement errors. Although there is a surprising laterality between

hemispheres with each age, this may be the result of processing hemispheres independently during image processing. This can also explain the lack of environmental correlations between homologous regions across hemispheres. The strong environmental correlations of the same region across time are more likely to be caused by some unknown environmental influence unique to everyone (Fig. 4c). Previous studies have shown that environmental influences from exercising (Voelcker-Rehage and Niemann 2013; López-Vicente et al. 2017), smoking and substance use (Jacobus et al. 2015; Karama et al. 2015), and prenatal exposure to aversive environment (Gautam et al. 2015; Marroun et al. 2016) can influence cortical thickness.

With a similar number of females and males in the study it was possible to assess differences between the sexes. We found negligible influences of sex, handedness, and age at scan on heritability of (changes) in cortical thickness in qualitative post-hoc analyses. Quantitative evaluation of sex and handedness effects on the means and variance of (changes in) global cortical thickness confirmed the absence of sex or handedness effects. Although sex effects for mean and variance of changes in cortical thickness between ages 12 and 17 years were approaching significance, no discernible effects were observed in the qualitative evaluation. It remains unclear if sex differences in cortical thickness during development exist (Lenroot and Giedd 2010; Walhovd et al. 2017). Our longitudinal data on cortical thickness development reveals no sex differences in global cortical thickness across childhood and adolescent development (Fig. 3).

This study has several limitations which should be taken into consideration when interpreting its findings. One, the bivariate twin analysis has a limited level of detail by using a lobar segmentation of the cortex. Although genetic clustering of the cortex appears to largely conform to anatomical boundaries defined by sulci and gyri, the genetically optimal configuration has a more refined subdivision of the cortical lobes (Chen et al. 2012; 2013; Peng et al. 2016; Wen et al. 2016). As a result, the use of a lobar segmentation may result in a mixture of different gene pools for each lobar region, which may impact our ability to detect distinct genetic factors between regions. Two, the statistical power of a twin study determines the effect sizes than can be detected (Posthuma and Boomsma 2000; Panizzon et al. 2009) and our sample is modest for twin modeling purposes. The longitudinal design of this study increases the power substantially for heritability estimates of measures correlated across time such as cortical thickness, while the ability to detect genetic innovation depends on nonshared genetic factors influencing the individual measures (i.e., genetic factors influences both measures are not perfectly correlated). Thus, there is a balance being able to detect heritability and being able to detect genetic innovation depending on the amount of genetic overlap between the variables. Assuming a ground truth based on the phenotypic covariance matrix for mean global cortical thickness from our own data, a post-hoc simulation study detected significant heritability of cortical thickness at all 3 waves and heritability of cortical thickness change with a power between 90% and 100%. However, it must be noted that we are underpowered to detect genetic innovation: genetic innovation at age 12 years was detected in 59% of the simulation runs, and at age 17 years in only in 26% of the simulation runs. Three, with a 5-year interval between age 12 and 17 years compared with a 3-year interval between age 9 and 12 years, we expected to see increased sensitivity for heritability estimates of changes in cortical thickness since more time has passed to allow for changes in cortical thickness to occur and consequently an increased variance between individuals. This increased sensitivity is enhanced by the increased rate of changes in cortical thickness during the second half of adolescence. Indeed, we found larger areas significant for heritability of changes in cortical thickness between age 12 and 17 years than between age 9 and 12 years (Fig. 5). With a 5-fold increase in additive genetic variance for changes in cortical thickness between age 12 and 17 years compared with only 2-fold increase in phenotypic variance and no changes to environmental variance, we believe the increased heritability of changes in cortical thickness between age 12 and 17 years can be attributed to increased rate of cortical thinning and not merely to the difference in time interval between scans. Despite the increase in sensitivity to detect changes between age 12 and 17 years, we found fewer and smaller clusters with genetic innovation than between age 9 and 12 years (Fig. 5*b* and Table 1).

Despite its limitations, the longitudinal design of this study with its strict age range at each measurement is ideally suited for the longitudinal twin analysis investigating heritability of changes in cortical thickness since it permits exploiting rules of variance to readily obtain covariance matrices for change measures without having to consider a diverse range of ages of the participants. Slight variations in individuals' scan interval, implicitly modeled by incorporating *age at scan* as variable of no interest in the post-hoc analysis, did not have any discernible effect on the results.

In conclusion, cortical thickness development during childhood and adolescence is under strong genetic control and although it is largely driven by a single genetic factor, the influence exerted by this core genetic factor varies with age and its influence seems to decrease towards adulthood. In addition, new genetic factors influence regional cortical thickness development during different stages of childhood and adolescent development. These new genetic factors might explain the rapid cognitive and behavioral development during adolescence and could potentially be associated with the manifestation of psychiatric disorders during adolescence.

Supplementary Material

Supplementary material is available at *Cerebral Cortex* online.

Funding

This work was supported by Nederlandse Organisatie voor Wetenschappelijk Onderzoek (NWO 51.02.061 to H.H., NWO 51.02.062 to D.B., NWO-NIHC Programs of excellence 433-09-220 to H.H., NWO-MagW 480-04-004 to D.B., and NWO/SPI 56-464-14192 to D.B.); FP7 Ideas: European Research Council (ERC-230374 to D.B.); and Universiteit Utrecht (High Potential Grant to H.H.); and Ministerie van Onderwijs, Cultuur en Wetenschap and Nederlandse Organisatie voor Wetenschappelijk Onderzoek (NWO 024.001.003 to Consortium on Individual Development).

Availability of data and code

Requests for access to the data and code used in this analysis should be directed to the corresponding author. Definitions of the bivariate and longitudinal structural equation models in OpenMx are provided as supplementary files.

Notes

We would like to thank the twins and their parents for making this study possible. *Conflict of Interest*: None declared.

References

Akbarian S, Liu C, Knowles JA, Vaccarino FM, Farnham PJ, Crawford GE, Jaffe AE, Pinto D, Dracheva S, Geschwind DH, et al. 2015. The PsychENCODE project. Nat. Hum Behav. 18: 1707–1712.

Alexander-Bloch AF, Giedd JN, Bullmore ET. 2013. Imaging structural co-variance between human brain regions. Nat Rev Neurosci. 14:322–336.

Blokland GAM, de Zubicaray GI, McMahon KL, Wright MJ. 2012. Genetic and environmental influences on neuroimaging phenotypes: a meta-analytical perspective on twin imaging studies. Twin Res Hum Genet. 15:351–371.

Boker SM, Neale MC, Maes HH, Wilde MJ, Spiegel M, Brick TR, Estabrook R, Bates TC, Mehta P, Oertzen von T, et al 2015. OpenMX 2.2.6 User Guide.

Boomsma DI, Busjahn A, Peltonen L. 2002. Classical twin studies and beyond. Nat Rev Genet. 3:872–882.

Boomsma DI, de Geus EJC, Vink JM, Stubbe JH, Distel MA, Hottenga J-J, Posthuma D, van Beijsterveldt CEM, Hudziak JJ, Bartels M, et al. 2006. Netherlands Twin Register: from twins to twin families. Twin Res Hum Genet. 9:849–857.

Bourgeois JP, Rakic P. 1993. Changes of synaptic density in the primary visual cortex of the macaque monkey from fetal to adult stage. J Neurosci. 13:2801–2820.

Brans RGH, Kahn RS, Schnack HG, van Baal GCM, Posthuma D, van Haren NEM, Lepage C, Lerch JP, Collins DL, Evans AC, et al. 2010. Brain plasticity and intellectual ability are influenced by shared genes. J Neurosci. 30:5519–5524.

Brouwer RM, Hulshoff Pol HE, Schnack HG. 2010. Segmentation of MRI brain scans using non-uniform partial volume densities. Neuroimage. 49:467–477.

Chen C-H, Fiecas MJA, Gutiérrez ED, Panizzon MS, Eyler LT, Vuoksimaa E, Thompson WK, Fennema-Notestine C, Hagler DJ, Jernigan TL, et al. 2013. Genetic topography of brain morphology. Proc Natl Acad Sci USA. 110:17089–17094.

Chen C-H, Gutiérrez ED, Thompson W, Panizzon MS, Jernigan TL, Eyler LT, Fennema-Notestine C, Jak AJ, Neale MC, Franz CE, et al. 2012. Hierarchical genetic organization of human cortical surface area. Science. 335:1634–1636.

Colantuoni C, Lipska BK, Ye T, Hyde TM, Tao R, Leek JT, Colantuoni EA, Elkahloun AG, Herman MM, Weinberger DR, et al. 2011. Temporal dynamics and genetic control of transcription in the human prefrontal cortex. Nature. 478: 519–523.

Dekaban AS, Sadowsky D. 1978. Changes in brain weights during the span of human life: relation of brain weights to body heights and body weights. Ann Neurol. 4:345–356.

den Braber A, Bohlken MM, Brouwer RM, van 't Ent D, Kanai R, Kahn RS, de Geus EJC, Hulshoff Pol HE, Boomsma DI. 2013. Heritability of subcortical brain measures: a perspective for future genome-wide association studies. NeuroImage. 83: 98–102.

Deoni SCL, Dean DC, Remer J, Dirks H, O'Muircheartaigh J. 2015. Cortical maturation and myelination in healthy toddlers and young children. Neuroimage. 115:147–161.

Docherty AR, Sawyers CK, Panizzon MS, Neale MC, Eyler LT, Fennema-Notestine C, Franz CE, Chen C-H, McEvoy LK, Verhulst B, et al. 2015. Genetic network properties of the human cortex based on regional thickness and surface area measures. Front Hum Neurosci. 9:1–14.

Dominicus A, Skrondal A, Gjessing HK, Pedersen NL, Palmgren J. 2006. Likelihood ratio tests in behavioral genetics: problems and solutions. Behav Genet. 36:331–340.

Douet V, Chang L, Cloak C, Ernst TM. 2014. Genetic influences on brain developmental trajectories on neuroimaging studies: from infancy to young adulthood. Brain Imaging Behav. 8:234–250.

El Marroun H, Tiemeier H, Franken IHA, Jaddoe VWV, van der Lugt A, Verhulst FC, Lahey BB, White TJH. 2016. Prenatal cannabis and tobacco exposure in relation to brain morphology: a prospective neuroimaging study in young children. Biol Psychiatry. 79:971–979.

Eyler LT, Chen C-H, Panizzon MS, Fennema-Notestine C, Neale MC, Jak AJ, Jernigan TL, Fischl B, Franz CE, Lyons MJ, et al. 2012. A comparison of heritability maps of cortical surface area and thickness and the influence of adjustment for whole brain measures: a magnetic resonance imaging twin study. Twin Res Hum Genet. 15:304–314.

Falconer DS, Mackay TFC. 1996. Introduction to quantitative genetics. 4th ed. Amsterdam, The Netherlands: Pearson.

Fjell AM, Grydeland H, Krogsrud SK, Amlien IK, Rohani DA, Ferschmann L, Storsve AB, Tamnes CK, Sala-Llonch R, Due-Tønnessen P, et al. 2015. Development and aging of cortical thickness correspond to genetic organization patterns. Proc Natl Acad Sci USA. 112:15462–15467.

Gautam P, Warner TD, Kan EC, Sowell ER. 2015. Executive function and cortical thickness in youths prenatally exposed to cocaine, alcohol and tobacco. Dev Cogn Neurosci. 16:155–165.

Genovese CR, Lazar NA, Nichols TE. 2002. Thresholding of statistical maps in functional neuroimaging using the false discovery rate. NeuroImage. 15:870–878.

Giedd JN, Blumenthal JD, Jeffries NO, Castellanos FX, Liu H, Zijdenbos AP, Paus T, Evans AC, Rapoport JL. 1999. Brain development during childhood and adolescence: a longitudinal MRI study. Nat Neurosci. 2:861–863.

Giedd JN, Raznahan A, Alexander-Bloch AF, Schmitt E, Gogtay N, Rapoport JL. 2015. Child psychiatry branch of the National Institute of Mental Health longitudinal structural magnetic resonance imaging study of human brain development. Neuropsychopharmacology. 40:43–49.

Giedd JN, Stockman M, Weddle C, Liverpool M, Alexander-Bloch AF, Wallace GL, Lee NR, Lalonde F, Lenroot RK. 2010. Anatomic magnetic resonance imaging of the developing child and adolescent brain and effects of genetic variation. Neuropsychol Rev. 20:349–361.

Gogtay N, Giedd JN, Lusk L, Hayashi KM, Greenstein DK, Vaituzis AC, Nugent TF, Herman DH, Clasen LS, Toga AW, et al. 2004. Dynamic mapping of human cortical development during childhood through early adulthood. Proc Natl Acad Sci USA. 101:8174–8179.

Greenstein DK, Lerch JP, Shaw PW, Clasen LS, Giedd JN, Gochman P, Rapoport JL, Gogtay N. 2006. Childhood onset schizophrenia: cortical brain abnormalities as young adults. J Child Psychol Psychiatry. 47:1003–1012.

Hawrylycz M, Miller JA, Menon V, Feng D, Dolbeare T, Guillozet-Bongaarts AL, Jegga AG, Aronow BJ, Lee C-K, Bernard A, et al. 2015. Canonical genetic signatures of the adult human brain. Nat Neurosci. 18:1832–1844.

Hedman AM, van Haren NEM, Schnack HG, Kahn RS, Hulshoff Pol HE. 2011. Human brain changes across the life span: a review of 56 longitudinal magnetic resonance imaging studies. Hum Brain Mapp. 33:1987–2002.

Hedman AM, van Haren NEM, van Baal GCM, Brouwer RM, Brans RGH, Schnack HG, Kahn RS, Hulshoff Pol HE. 2016. Heritability of cortical thickness changes over time in twin pairs discordant for schizophrenia. Schizophr Res. 173: 192–199.

Hulshoff Pol HE, Schnack HG, Posthuma D, Mandl RCW, Baaré WFC, van Oel CJ, van Haren NEM, Collins DL, Evans AC, Amunts K, et al. 2006. Genetic contributions to human brain morphology and intelligence. J Neurosci. 26:10235–10242.

Huttenlocher PR. 1979. Synaptic density in human frontal cortex – developmental changes and effects of aging. Brain Res. 163:195–205.

Huttenlocher PR, Dabholkar AS. 1997. Regional differences in synaptogenesis in human cerebral cortex. J Comp Neurol. 387:167–178.

Jacobus J, Squeglia LM, Meruelo AD, Castro N, Brumback T, Giedd JN, Tapert SF. 2015. Cortical thickness in adolescent marijuana and alcohol users: a three-year prospective study from adolescence to young adulthood. Dev Cogn Neurosci. 16:101–109.

Jaffe AE, Shin J, Collado-Torres L, Leek JT, Tao R, Li C, Gao Y, Jia Y, Maher BJ, Hyde TM, et al. 2015. Developmental regulation of human cortex transcription and its clinical relevance at single base resolution. Nat Hum Behav. 18:154–161.

Jansen AG, Mous SE, White TJH, Posthuma D, Polderman TJC. 2015. What twin studies tell us about the heritability of brain development, morphology, and function: a review. Neuropsychol Rev. 25:27–46.

Jeon S, Lepage C, Lewis L, Khalili-Mahani N, Bermudez P, Vincent R, Zijdenbos AP, Omidyeganeh M, Adalat R, Evans AC 2017. Reproducibility of Cortical Thickness Measurement: CIVET (v2.1) vs. Freesurfer (v6.0-beta & v5.3). On Human Brain Mapping Symposium.

Kang HJ, Kawasawa YI, Cheng F, Zhu Y, Xu X, Li M, Sousa AMM, Pletikos M, Meyer KA, Sedmak G, et al. 2011. Spatio-temporal transcriptome of the human brain. Nature. 478: 483–489.

Karama S, Ducharme S, Corley J, Chouinard-Decorte F, Starr JM, Wardlaw JM, Bastin ME, Deary IJ. 2015. Cigarette smoking and thinning of the brain's cortex. Mol Psychiatry. 20: 778–785.

Kim JS, Singh V, Lee JK, Lerch JP, Ad-Dab'bagh Y, MacDonald D, Lee JM, Kim SI, Evans AC. 2005. Automated 3-D extraction and evaluation of the inner and outer cortical surfaces using a Laplacian map and partial volume effect classification. Neuroimage. 27:210–221.

Kramer AF, Bherer L, Colcombe SJ, Dong W, Greenough WT. 2004. Environmental influences on cognitive and brain plasticity during aging. J Gerontol A Biol Sci Med Sci. 59: 940–957.

Lenroot RK, Giedd JN. 2008. The changing impact of genes and environment on brain development during childhood and adolescence: initial findings from a neuroimaging study of pediatric twins. Dev Psychopathol. 20:1161–1175.

Lenroot RK, Giedd JN. 2010. Sex differences in the adolescent brain. Brain Cognit. 72:46–55.

Lenroot RK, Schmitt JE, Ordaz SJ, Wallace GL, Neale MC, Lerch JP, Kendler KS, Evans AC, Giedd JN. 2009. Differences in genetic and environmental influences on the human cerebral cortex associated with development during childhood and adolescence. Hum Brain Mapp. 30:163–174.

Lerch JP, Pruessner J, Zijdenbos AP, Collins DL, Teipel SJ, Hampel H, Evans AC. 2008. Automated cortical thickness measurements from MRI can accurately separate Alzheimer's patients from normal elderly controls. Neurobiol Aging. 29: 23–30.

Lewis L, Lepage C, Khalili-Mahani N, Omidyeganeh M, Jeon S, Bermudez P, Zijdenbos AP, Vincent R, Adalat R, Evans AC 2017. Robustness and reliability of cortical surface reconstruction in CIVET and FreeSurfer. On Human Brain Mapping Symposium.

Lyttelton O, Boucher M, Robbins S, Evans AC. 2007. An unbiased iterative group registration template for cortical surface analysis. Neuroimage. 34:1535–1544.

López-Vicente M, Tiemeier H, Wildeboer A, Muetzel RL, Verhulst FC, Jaddoe VWV, Sunyer J, White TJH. 2017. Cortical structures associated with sports participation in children: a population-based study. Dev Neuropsychol. 42:58–69.

Maechler M, Rousseeuw PJ, Struyf A, Hubert M, Hornik K. 2016. cluster: Cluster Analysis Basics and Extensions.

Miller DJ, Duka T, Stimpson CD, Schapiro SJ, Baze WB, McArthur MJ, Fobbs AJ, Sousa AMM, Sestan N, Wildman DE, et al. 2012. Prolonged myelination in human neocortical evolution. Proc Natl Acad Sci USA. 109:16480–16485.

Mills KL, Goddings A-L, Herting MM, Meuwese R, Blakemore S-J, Crone EA, Dahl RE, Güroğlu B, Raznahan A, Sowell ER, et al. 2016. Structural brain development between childhood and adulthood: convergence across four longitudinal samples. Neuroimage. 141:273–281.

Mills KL, Tamnes CK. 2014. Methods and considerations for longitudinal structural brain imaging analysis across development. Dev Cogn Neurosci. 9:172–190.

Naumova OY, Lee M, Rychkov SY, Vlasova NV, Grigorenko EL. 2013. Gene expression in the human brain: the current state of the study of specificity and spatiotemporal dynamics. Child Dev. 84:76–88.

Panizzon MS, Fennema-Notestine C, Eyler LT, Jernigan TL, Prom-Wormley EC, Neale MC, Jacobson K, Lyons MJ, Grant MD, Franz CE, et al. 2009. Distinct genetic influences on cortical surface area and cortical thickness. Cereb Cortex. 19: 2728–2735.

Paus T. 2010. Growth of white matter in the adolescent brain: myelin or axon? Brain Cognition. 72:26–35.

Paus T, Keshavan MS, Giedd JN. 2008. Why do many psychiatric disorders emerge during adolescence? Nat Rev Neurosci. 9: 947–957.

Peng Q, Schork AJ, Bartsch H, Lo M-T, Panizzon MS, Pediatric Imaging, Neurocognition and Genetics Study, Alzheimer's Disease Neuroimaging Initiative, Westlye LT, Kremen WS, Jernigan TL, Le Hellard S, Steen VM, Espeseth T, et al. 2016. Conservation of distinct genetically-mediated human cortical pattern. PLoS Genet. 12:1–18.

Peper JS, Brouwer RM, Boomsma DI, Kahn RS, Hulshoff Pol HE. 2007. Genetic influences on human brain structure: a review of brain imaging studies in twins. Hum Brain Mapp. 28: 464–473.

Peper JS, Brouwer RM, Schnack HG, van Baal GCM, van Leeuwen M, van den Berg SM, Delemarre-Van de Waal HA, Janke AL, Collins DL, Evans AC, et al. 2008. Cerebral white matter in early puberty is associated with luteinizing hormone concentrations. Psychoneuroendocrinology. 33:909–915.

Peper JS, Schnack HG, Brouwer RM, van Baal GCM, Pjetri E, Székely E, van Leeuwen M, van den Berg SM, Collins DL, Evans AC, et al. 2009. Heritability of regional and global brain structure at the onset of puberty: A magnetic resonance imaging study in 9-year-old twin pairs. Hum Brain Mapp. 30:2184–2196.

Petanjek Z, Judaš M, Šimic G, Rasin MR, Uylings HBM, Rakic P, Kostovic I. 2011. Extraordinary neoteny of synaptic spines in the human prefrontal cortex. Proc Natl Acad Sci USA. 108: 13281–13286.

Pinheiro J, Bates D, DebRoy S, Sarkar D, R Core Team. 2017. nlme: Linear and Nonlinear Mixed Effects Models.

Pletikos M, Sousa AMM, Sedmak G, Meyer KA, Zhu Y, Cheng F, Li M, Kawasawa YI, Sestan N. 2014. Temporal specification and bilaterality of human neocortical topographic gene expression. Neuron. 81:321–332.

Posthuma D, Boomsma DI. 2000. A note on the statistical power in extended twin designs. Behav Genet. 30:147–158.

Posthuma D, de Geus EJC, Neale MC, Hulshoff Pol HE, Baaré WFC, Kahn RS, Boomsma DI. 2000. Multivariate genetic analysis of brain structure in an extended twin design. Behav Genet. 30:311–319.

R Core Team. 2015. R: A Language and Environment for Statistical Computing version 3.2.2.

Rapoport JL, Gogtay N. 2008. Brain neuroplasticity in healthy, hyperactive and psychotic children: insights from neuroimaging. Neuropsychopharmacology. 33:181–197.

Raznahan A, Lerch JP, Lee N, Greenstein D, Wallace GL, Stockman M, Clasen LS, Shaw PW, Giedd JN. 2011a. Patterns of coordinated anatomical change in human cortical development: a longitudinal neuroimaging study of maturational coupling. Neuron. 72:873–884.

Raznahan A, Shaw PW, Lalonde F, Stockman M, Wallace GL, Greenstein D, Clasen LS, Gogtay N, Giedd JN. 2011b. How does your cortex grow? J Neurosci. 31:7174–7177.

Redolfi A, Manset D, Barkhof F, Wahlund L-O, Glatard T, Mangin J-F, Frisoni GB, neuGRID Consortium for the Alzheimer's Disease Neuroimaging Initiative. 2015. Head-to-head comparison of two popular cortical thickness extraction algorithms: a cross-sectional and longitudinal study. PLoS ONE. 10:e0117692.

Rimol LM, Panizzon MS, Fennema-Notestine C, Eyler LT, Fischl B, Franz CE, Hagler DJ, Lyons MJ, Neale MC, Pacheco J, et al. 2010. Cortical thickness is influenced by regionally specific genetic factors. Biol Psychiatry. 67:493–499.

Roth RB, Hevezi P, Lee J, Willhite D, Lechner SM, Foster AC, Zlotnik A. 2006. Gene expression analyses reveal molecular relationships among 20 regions of the human CNS. Neurogenetics. 7:67–80.

Rousseeuw PJ. 1987. Silhouettes: a graphical aid to the interpretation and validation of cluster analysis. J Comput Appl Math. 20:53–65.

Schmitt JE, Giedd JN, Raznahan A, Neale MC. 2017. The genetic contributions to maturational coupling in the human cerebrum: a longitudinal pediatric twin imaging study. Cereb Cortex. 1–8. doi:10.1093/cercor/bhx190.

Schmitt JE, Lenroot RK, Wallace GL, Ordaz SJ, Taylor KN, Kabani NJ, Greenstein DK, Lerch JP, Kendler KS, Neale MC, et al. 2008. Identification of genetically mediated cortical networks: a multivariate study of pediatric twins and siblings. Cereb Cortex. 18:1737–1747.

Schmitt JE, Neale MC, Fassassi B, Perez J, Lenroot RK, Wells EM, Giedd JN. 2014. The dynamic role of genetics on cortical patterning during childhood and adolescence. Proc Natl Acad Sci USA. 111:6774–6779.

Schnack HG, van Haren NEM, Brouwer RM, Evans AC, Durston S, Boomsma DI, Kahn RS, Hulshoff Pol HE. 2015. Changes in thickness and surface area of the human cortex and their relationship with intelligence. Cereb Cortex. 25:1608–1617.

Schnack HG, van Haren NEM, Nieuwenhuis M, Hulshoff Pol HE, Kahn RS. 2016. Accelerated brain aging in schizophrenia: a longitudinal pattern recognition study. Am J Psychiatry. 173:607–616.

Shaw PW, Eckstrand K, Sharp W, Blumenthal JD, Lerch JP, Greenstein DK, Clasen LS, Evans AC, Giedd JN, Rapoport JL. 2007. Attention-deficit/hyperactivity disorder is characterized by a delay in cortical maturation. Proc Natl Acad Sci USA. 104:19649–19654.

Shaw PW, Gogtay N, Rapoport JL. 2010. Childhood psychiatric disorders as anomalies in neurodevelopmental trajectories. Hum Brain Mapp. 31:917–925.

Silbereis JC, Pochareddy S, Zhu Y, Li M, Sestan N. 2016. The cellular and molecular landscapes of the developing human central nervous system. Neuron. 89:248–268.

Sled JG, Zijdenbos AP, Evans AC. 1998. A nonparametric method for automatic correction of intensity nonuniformity in MRI data. IEEE T Med Imaging. 17:87–97.

Somel M, Guo S, Fu N, Yan Z, Hu HY, Xu Y, Yuan Y, Ning Z, Hu Y, Menzel C, et al. 2010. MicroRNA, mRNA, and protein expression link development and aging in human and macaque brain. Genome Res. 20:1207–1218.

Sowell ER, Peterson BS, Kan E, Woods RP, Yoshii J, Bansal R, Xu D, Zhu H, Thompson PM, Toga AW. 2007. Sex differences in cortical thickness mapped in 176 healthy individuals between 7 and 87 years of age. Cereb Cortex. 17:1550–1560.

Storsve AB, Fjell AM, Tamnes CK, Westlye LT, Overbye K, Aasland HW, Walhovd KB. 2014. Differential longitudinal changes in cortical thickness, surface area and volume across the adult life span: regions of accelerating and decelerating change. J Neurosci. 34:8488–8498.

Strike LT, Couvy-Duchesne B, Hansell NK, Cuellar-Partida G, Medland SE, Wright MJ. 2015. Genetics and brain morphology. Neuropsychol Rev. 25:63–96.

Thompson PM, Cannon TD, Narr KL, van Erp TGM, Poutanen VP, Huttunen M, Lönnqvist J, Standertskjöld-Nordenstam CG, Kaprio J, Khaledy M, et al. 2001. Genetic influences on brain structure. Nat Neurosci. 4:1253–1258.

Tzourio-Mazoyer NEA, Landeau B, Papathanassiou D, Crivello F, Etard O, Delcroix N, Mazoyer B, Joliot M. 2002. Automated anatomical labeling of activations in SPM using a macroscopic anatomical parcellation of the MNI MRI single-subject brain. NeuroImage. 15:273–289.

van Beijsterveldt CEM, Groen-Blokhuis M, Hottenga J-J, Franić S, Hudziak JJ, Lamb D, Huppertz C, de Zeeuw E, Nivard MG, Schutte N, et al. 2013. The Young Netherlands Twin Register (YNTR): longitudinal twin and family studies in over 70,000 children. Twin Res Hum Genet. 16:252–267.

van Soelen ILC, Brouwer RM, Peper JS, van Leeuwen M, Koenis MMG, van Beijsterveldt CEM, Swagerman SC, Kahn RS, Hulshoff Pol HE, Boomsma DI. 2012a. Brain SCALE: brain structure and cognition: an adolescent longitudinal twin study into the genetic etiology of individual differences. Twin Res Hum Genet. 15:453–467.

van Soelen ILC, Brouwer RM, van Baal GCM, Schnack HG, Peper JS, Chen L, Kahn RS, Boomsma DI, Hulshoff Pol HE. 2013. Heritability of volumetric brain changes and height in children entering puberty. Hum Brain Mapp. 34:713–725.

van Soelen ILC, Brouwer RM, van Baal GCM, Schnack HG, Peper JS, Collins DL, Evans AC, Kahn RS, Boomsma DI, Hulshoff Pol HE. 2012b. Genetic influences on thinning of the cerebral cortex during development. NeuroImage. 59:3871–3880.

Voelcker-Rehage C, Niemann C. 2013. Structural and functional brain changes related to different types of physical activity across the life span. Neurosci Biobehav Rev. 37:2268–2295.

Walhovd KB, Fjell AM, Giedd JN, Dale AM, Brown TT. 2017. Through thick and thin: a need to reconcile contradictory results on trajectories in human cortical development. Cereb Cortex. 27:1472–1481.

Wei T, Simko V 2016. corrplot: Visualization of a Correlation Matrix version 0.77.

Wen W, Thalamuthu A, Mather KA, Zhu W, Jiang J, de Micheaux PL, Wright MJ, Ames D, Sachdev PS. 2016. Distinct genetic influences on cortical and subcortical brain structures. Sci Rep. 6:1–11.

Whitaker KJ, Vértes PE, Romero-Garcia R, Váša F, Moutoussis M, Prabhu G, Weiskopf N, Callaghan MF, Wagstyl K, Rittman T, et al. 2016. Adolescence is associated with genomically patterned consolidation of the hubs of the human brain connectome. Proc Natl Acad Sci USA. 113:9105–9110.

Zatorre RJ, Fields RD, Johansen-Berg H. 2012. Plasticity in gray and white: neuroimaging changes in brain structure during learning. Nat Hum Behav. 15:528–536.

Zielinski BA, Prigge MBD, Nielsen JA, Froehlich AL, Abildskov TJ, Anderson JS, Fletcher PT, Zygmunt KM, Travers BG, Lange N, et al. 2014. Longitudinal changes in cortical thickness in autism and typical development. Brain. 137:1799–1812.